XLIII CILAMCE
21–25, November, 2022
FOZ DO IGUAÇU – PR – BRAZIL

TOPOLOGY OPTIMIZATION OF CONTINUUM ELASTIC STRUCTURES EMPLOYING THE FINITE-VOLUME THEORY AND THE EVOLUTIONARY STRUCTURAL OPTIMIZATION METHOD

Luiz C. L. Véras[1], Márcio A. A. Cavalcante[2]

[1]*Center of Technology, Federal University of Alagoas*
Av. Lourival Melo Mota, Maceió, 57072-900, Alagoas, Brazil
luiz.veras@ctec.ufal.br
[2]*Campus of Engineering and Agricultural Sciences, Federal University of Alagoas*
BR-104, Rio Largo, 57100-000, Alagoas, Brazil
marcio.cavalcante@ceca.ufal.br

Abstract. In this paper, an original approach that combines Finite-Volume Theory (FVT) and Evolutionary Structural Optimization (ESO) is presented. ESO is based on the simple idea that the optimal structure can be delivered by gradually removing the ineffectively used material from the design domain. Through this procedure, the resulting structure will evolve towards its optimal shape and topology. In theory, one cannot guarantee that such an evolutionary procedure would always generate the best solution. However, the ESO technique provides a useful way for designers to explore forms and shapes of structures during the conceptual design stage. In literature, it is frequent that the design domain is constructed aiming at a Finite Element Analysis (FEA). However, some problems are related to numerical issues, such as the checkerboard pattern and mesh dependence. The checkboard effect is related to the assumptions of the finite element method, as the satisfaction of equilibrium and continuity conditions in the element nodes. FVT overcomes this problem because it satisfies the equilibrium equations at the subvolume level and the compatibility conditions are established through the adjacent subvolume interfaces, as expected from the continuum mechanics point of view. Some ESO's classical problems are investigated to compare FVT and FEA results.

Keywords: topology optimization; finite-volume theory; ESO.

1 Introduction

Several methods of structural topology optimization have been developed in recent decades, with important advances that have enabled practical applications. The ESO method initially proposed by Xie and Steven [1] is built on a pure heuristic principle that removes inefficient materials, and the structure evolves towards an optimum. Originally, ESO was implemented solely as a material removal method, which meant that removed parts could not be restored afterwards.

Xia *et al*. [2] mention that, since the early development of ESO method is based on a heuristic concept and lacks theoretical rigor, most of the early work on ESO neglected significant numerical problems in TO, such as the existence of a solution, checkerboard, mesh-dependency, and local optimum.

A checkerboard pattern describes a region alternating solid and void elements in a topology and it is commonly found in optimal solutions. It has been proven that the formation of the checkerboards is due to numerical instability and does not represent an optimal feature of the design. This problem appears commonly in most applications using the finite element method (FEM). The finite-volume theory (FVT) can reduce the checkerboard with no filtering techniques [3].

This work presents a new approach for TO of two-dimensional continuum elastic structures through the classic ESO method and FVT. The ESO is demonstrated on two ways: total strain energy-based and average von Mises

stress-based topology optimization problem. A classic bidimensional cantilever beam example is analyzed applying finite-volume theory to define the optimum design.

2 Evolutionary Structural Optimization (ESO)

The main ESO stress-based procedure is presented by Steven and Xie [4], so this work followed the central idea of that work. In addition to the von Mises equivalent stress, the total strain energy will be used as a performance criterion for selecting the subvolumes.

In the ESO algorithm, some parameters are essential and are defined as initial rejection ratio (RR_0), evolutionary rate (ER), rejection criterion (RC) and penalty factor (PF). The first three are defined in the classic ESO approach. In the case of continuous two-dimensional elastic structures, it is necessary to apply a PF to the stiffness matrix of the elements eliminated from the analyzed discretized domain, to avoid remeshing and singularity of the global stiffness matrix. In practice, values in the magnitude of 10^{-6} are recommended for the penalty factor.

Figure 1 shows the flowchart that summarizes all the steps for developing the ESO algorithm used in this work.

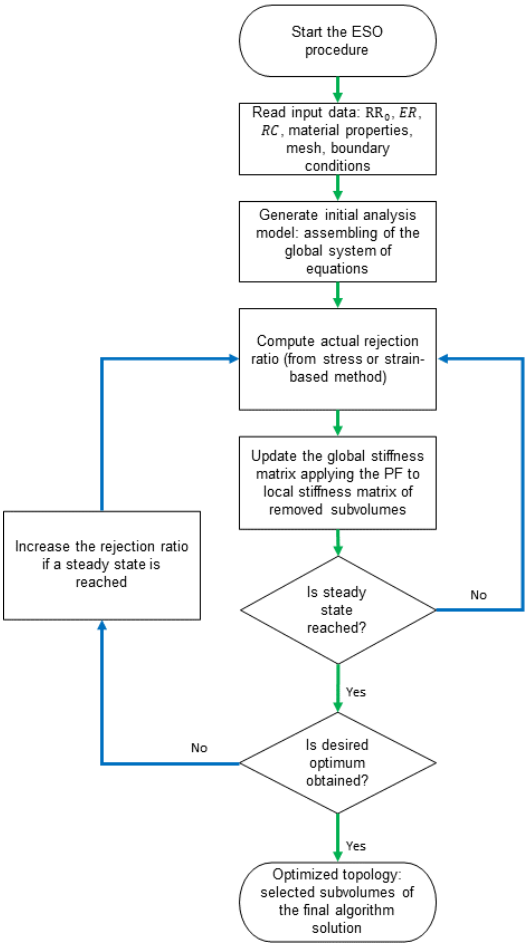

Figure 1. Flowchart of ESO algorithm.

3 Zero-Order Finite-Volume Theory

The present formulation has its roots in the Finite-Volume Theory (FVT) for bidimensional linear elastic structures developed by Bansal and Pindera [5]. The adopted reference domain is rectangular in $x_1 - x_2$ plane with $0 \leq x_1 \leq L$ and $0 \leq x_2 \leq H$, which is discretized in N_β horizontal subvolumes and N_γ vertical subvolumes, Fig. 2. The subvolume dimensions are designated by l_q and h_q for $q = 1, \ldots, N_q$, where $N_q = N_\beta \cdot N_\gamma$ is the total number of subvolumes. In this formulation, the components of the displacement field can be approximated by a Legendre polynomial expansion in the local coordinated system, as presented by Bansal and Pindera [5]:

$$u_i^{(q)} = W_{i(00)}^{(q)} + x_1^{(q)} W_{i(10)}^{(q)} + x_2^{(q)} W_{i(01)}^{(q)} + \frac{1}{2}\left(3{x_1^{(q)}}^2 - \frac{l_q^2}{4}\right) W_{i(20)}^{(q)} + \frac{1}{2}\left(3{x_2^{(q)}}^2 - \frac{h_q^2}{4}\right) W_{i(02)}^{(q)} \tag{1}$$

where $i = 1{,}2$ and $W_{i(mn)}^{(q)}$ are the unknown coefficients.

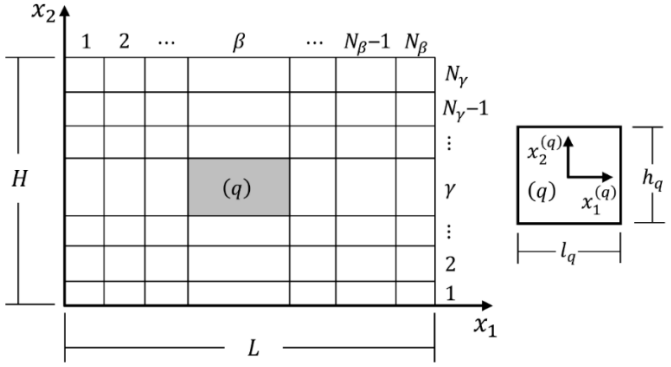

Figure 2. Discretized structure in rectangular subvolumes and local coordinate system of a generic subvolume q.

The coefficients of the local displacement field can be expressed as a function of the surface-averaged displacements. The surface-averaged displacements are defined as

$$\bar{u}_i^{(1,3)} = \frac{1}{l_q} \int_{-\frac{l_q}{2}}^{\frac{l_q}{2}} u_i\left(x_1^{(q)}, \mp\frac{h_q}{2}\right) dx_1^{(q)}$$
$$\bar{u}_i^{(2,4)} = \frac{1}{h_q} \int_{-\frac{h_q}{2}}^{\frac{h_q}{2}} u_i\left(\pm\frac{l_q}{2}, x_2^{(q)}\right) dx_2^{(q)} \tag{2}$$

where the superscript indicates the subvolume face number, indexed as illustrated in Fig. 3.

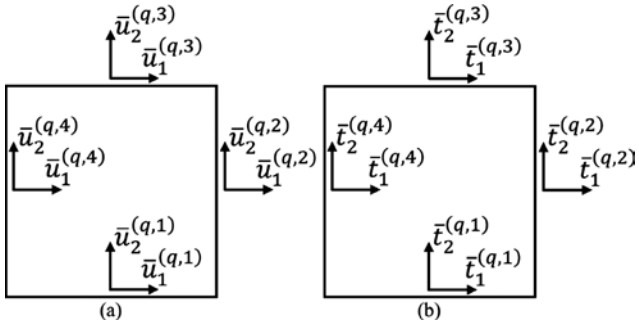

Figure 3. Surface-averaged kinematic and static quantities for a generic subvolume q: (a) surface-averaged displacements and (b) surface-averaged tractions.

The surface-averaged tractions acting on the subvolume's faces are defined as

$$\bar{t}_i^{(1,3)} = \mp\frac{1}{l_q} \int_{-\frac{l_q}{2}}^{\frac{l_q}{2}} \sigma_{2i}\left(x_1^{(q)}, \mp\frac{h_q}{2}\right) dx_1^{(q)}$$
$$\bar{t}_i^{(2,4)} = \pm\frac{1}{h_q} \int_{-\frac{h_q}{2}}^{\frac{h_q}{2}} \sigma_{1i}\left(\pm\frac{l_q}{2}, x_2^{(q)}\right) dx_2^{(q)} \tag{3}$$

Following Araujo *et al*. [3], the local system of equations for a generic subvolume can be stated as

$$\bar{\boldsymbol{t}}^{(q)} = \boldsymbol{K}^{(q)}_{(8\times8)}\bar{\boldsymbol{u}}^{(q)} \tag{4}$$

where $\bar{\boldsymbol{t}}^{(q)}$ is the local surface-averaged traction vector, $\boldsymbol{K}^{(q)}_{(8\times8)}$ is the local stiffness matrix and $\bar{\boldsymbol{u}}^{(q)}$ is the local surface-averaged displacement vector.

For the global stiffness matrix assemblage, the individual contribution of each subvolume in the discretized structure is considered. Therefore, the global system of equations can be defined as

$$\boldsymbol{T}_{(ndof\times1)} = \boldsymbol{K}_{(ndof\times ndof)}\boldsymbol{U}_{(ndof\times1)} \tag{5}$$

where $ndof$ is the number of degrees of freedom, $\boldsymbol{T}_{(ndof\times1)}$ and $\boldsymbol{U}_{(ndof\times1)}$ are the global surface-averaged traction and displacement vectors, respectively, and $\boldsymbol{K}_{(ndof\times ndof)}$ is the global stiffness matrix, which can be evaluated by

$$\boldsymbol{K}_{(ndof\times ndof)} = \sum_{q=1}^{N_q}\left[\left(\boldsymbol{L}^{(q)}_{(8\times ndof)}\right)^T \boldsymbol{K}^{(q)}_{(8\times8)}\boldsymbol{L}^{(q)}_{(8\times ndof)}\right] \tag{6}$$

where $\left(\boldsymbol{L}^{(q)}_{(8\times ndof)}\right)^T$ and $\boldsymbol{L}^{(q)}_{(8\times ndof)}$ are the static and kinematic incidence matrices of the subvolume *q*.

Now, to define the performance parameters that will be used to obtain the optimal topology of the structure, the following sections are presented as obtaining the total strain energy and the average von Mises stress from the FVT.

More details about FVT can be found in M. A. A. Cavalcante and M. J. Pindera [7] and [8].

3.1 Total Strain Energy

Araujo *et al*. [6] show that, as in the finite element method, the zeroth-order finite-volume theory satisfies the energy balance, i.e., the equality between the work done by external loading and the total strain energy. The total strain energy for the FVT can be evaluated as follows,

$$U = \sum_{q=1}^{N_q} U_q = \sum_{q=1}^{N_q}\left[\boldsymbol{L}^{(q)}\bar{\boldsymbol{t}}^{(q)}\right]^T\bar{\boldsymbol{u}}^{(q)} = \sum_{q=1}^{N_q}\left[\boldsymbol{L}^{(q)}\boldsymbol{K}^{(q)}_{(8\times8)}\bar{\boldsymbol{u}}^{(q)}\right]^T\bar{\boldsymbol{u}}^{(q)} \tag{7}$$

where $\boldsymbol{L}^{(q)}$ is the matrix containing the subvolume face lengths being expressed as

$$\boldsymbol{L}^{(q)} = \begin{bmatrix} \boldsymbol{L}^{(q)}_{(1)} & \boldsymbol{0} & \boldsymbol{0} & \boldsymbol{0} \\ \boldsymbol{0} & \boldsymbol{L}^{(q)}_{(2)} & \boldsymbol{0} & \boldsymbol{0} \\ \boldsymbol{0} & \boldsymbol{0} & \boldsymbol{L}^{(q)}_{(3)} & \boldsymbol{0} \\ \boldsymbol{0} & \boldsymbol{0} & \boldsymbol{0} & \boldsymbol{L}^{(q)}_{(4)} \end{bmatrix} \text{ for } \boldsymbol{L}^{(q)}_{(p)} = \begin{bmatrix} L^{(q)}_p & 0 \\ 0 & L^{(q)}_p \end{bmatrix} \tag{8}$$

and $L^{(q)}_1 = l_q$, $L^{(q)}_2 = h_q$, $L^{(q)}_3 = l_q$ e $L^{(q)}_4 = h_q$ are the faces' lengths of the subvolume q.

3.2 Locally Applied Average Stress Theorem to the Finite Volume Theory

A proposal for evaluating the square of the average equivalent von Mises stress for each subvolume is presented below based on the average stress theorem of micromechanics. It is a much more efficient way to carry out this analysis, which is possible for the finite-volume theory because of the satisfaction of the differential equilibrium equations in the subvolumes. The average stress theorem is applied as presented below for the correct selection of the subvolumes that discretize a two-dimensional domain.

$$\frac{1}{V}\int_S t_i\cdot x_j\cdot dS = \frac{1}{V}\int_S \sigma_{ki}\cdot n_k\cdot x_j\cdot dS = \frac{1}{V}\int_V \sigma_{ki}\cdot\frac{\partial x_j}{\partial x_k}\cdot dV + \frac{1}{V}\int_V \frac{\partial\sigma_{ki}}{\partial x_k}\cdot x_j\cdot dV = \frac{1}{V}\int_V \sigma_{ji}\cdot dV + \frac{1}{V}\int_V \frac{\partial\sigma_{ki}}{\partial x_k}\cdot x_j\cdot dV = \bar{\sigma}_{ij} + \frac{1}{V}\int_V \frac{\partial\sigma_{ki}}{\partial x_k}\cdot x_j\cdot dV \tag{9}$$

where $\bar{\sigma}_{ij} = \frac{1}{V}\int_V \sigma_{ji}\cdot dV$ is the volume-averaged stress.

Thus,

$$\bar{\sigma}_{ij} = \frac{1}{V}\int_S t_i \cdot x_j \cdot dS - \frac{1}{V}\int_V \frac{\partial \sigma_{ki}}{\partial x_k} \cdot x_j \cdot dV \tag{10}$$

When the differential equilibrium equations are satisfied, in the absence of body forces:

$$\bar{\sigma}_{ij} = \frac{1}{V}\int_S t_i \cdot x_j \cdot dS \tag{11}$$

The presented formulation has its roots in the finite-volume theory, developed by Bansal and Pindera [5], for bidimensional linear elastic structures. From Eq. 1, strain field can be written as:

$$\begin{aligned} \varepsilon_{11}^{(q)} &= W_{1(10)}^{(q)} + 3x_1^{(q)} W_{1(20)}^{(q)} \\ \varepsilon_{22}^{(q)} &= W_{2(01)}^{(q)} + 3x_2^{(q)} W_{2(02)}^{(q)} \\ 2 \cdot \varepsilon_{12}^{(q)} &= W_{1(01)}^{(q)} + 3x_2^{(q)} W_{1(02)}^{(q)} + W_{2(10)}^{(q)} + 3x_1^{(q)} W_{2(20)}^{(q)} \end{aligned} \tag{12}$$

Then the stress field is defined as:

$$\begin{aligned} \sigma_{11}^{(q)} &= C_{11}^{(q)}\left(W_{1(10)}^{(q)} + 3x_1^{(q)} W_{1(20)}^{(q)}\right) + C_{12}^{(q)}\left(W_{2(01)}^{(q)} + 3x_2^{(q)} W_{2(02)}^{(q)}\right) \\ \sigma_{22}^{(q)} &= C_{12}^{(q)}\left(W_{1(10)}^{(q)} + 3x_1^{(q)} W_{1(20)}^{(q)}\right) + C_{11}^{(q)}\left(W_{2(01)}^{(q)} + 3x_2^{(q)} W_{2(02)}^{(q)}\right) \\ \sigma_{12}^{(q)} &= C_{44}^{(q)}\left(W_{1(01)}^{(q)} + 3x_2^{(q)} W_{1(02)}^{(q)} + W_{2(10)}^{(q)} + 3x_1^{(q)} W_{2(20)}^{(q)}\right) \end{aligned} \tag{13}$$

Using the Eq (2), the volume-averaged stress components are evaluated as follows:

$$\overline{\boldsymbol{\sigma}}^{(q)} = \begin{Bmatrix} \bar{\sigma}_{11} \\ \bar{\sigma}_{22} \\ \bar{\sigma}_{12} \end{Bmatrix} = \boldsymbol{T} \cdot \overline{\boldsymbol{t}}^{(\boldsymbol{q})} \tag{14}$$

where:

$$\boldsymbol{T} = \begin{bmatrix} 0 & 0 & 1/2 & 0 & 0 & 0 & -1/2 & 0 \\ 0 & -1/2 & 0 & 0 & 0 & 1/2 & 0 & 0 \\ -1/2 & 0 & 0 & 0 & 1/2 & 0 & 0 & 0 \end{bmatrix} \text{ and}$$

$\overline{\boldsymbol{t}}^{(\boldsymbol{q})} = \begin{bmatrix} \overline{t}_1^{(q,1)} & \overline{t}_2^{(q,1)} & \overline{t}_1^{(q,2)} & \overline{t}_2^{(q,2)} & \overline{t}_1^{(q,3)} & \overline{t}_2^{(q,3)} & \overline{t}_1^{(q,4)} & \overline{t}_2^{(q,4)} \end{bmatrix}^T$. $\overline{\boldsymbol{t}}^{(\boldsymbol{q})}$ is the surface-averaged traction vector of a subvolume $\boldsymbol{q}$, and $\boldsymbol{T}$ is a transformation matrix.

The square of the volume-averaged von Mises stress can be evaluated as follow

$$\overline{\sigma}_{vM}^2 = \overline{\boldsymbol{\sigma}}^{(q)^T} \cdot \boldsymbol{P} \cdot \overline{\boldsymbol{\sigma}}^{(q)} \tag{15}$$

where:

$$\boldsymbol{P} = \begin{bmatrix} 1 & -1/2 & 0 \\ -1/2 & 1 & 0 \\ 0 & 0 & 3 \end{bmatrix} \tag{16}$$

Thus,

$$\overline{\sigma}_{vM}^2 = \overline{\boldsymbol{t}}^{(q)^T} \cdot \boldsymbol{T}^T \cdot \boldsymbol{P} \cdot \boldsymbol{T} \cdot \overline{\boldsymbol{t}}^{(q)} \Rightarrow \overline{\sigma}_{vM} = \overline{\boldsymbol{u}}^{(q)^T} \cdot \boldsymbol{K}^{(q)^T} \cdot \overline{\boldsymbol{P}} \cdot \boldsymbol{K}^{(q)} \cdot \overline{\boldsymbol{u}}^{(q)} \tag{17}$$

where $\overline{\boldsymbol{u}}^{(\boldsymbol{q})} = \begin{bmatrix} \overline{u}_1^{(q,1)} & \overline{u}_2^{(q,1)} & \overline{u}_1^{(q,2)} & \overline{u}_2^{(q,2)} & \overline{u}_1^{(q,3)} & \overline{u}_2^{(q,3)} & \overline{u}_1^{(q,4)} & \overline{u}_2^{(q,4)} \end{bmatrix}^T$ is the surface-averaged displacement vector, $\overline{\mathbf{P}} = \boldsymbol{T}^T \cdot \mathbf{P} \cdot \boldsymbol{T}$ is an auxiliar symmetric matrix and $\boldsymbol{K}^{(\mathrm{q})}$ is the local stiffness matrix of a generic subvolume $\boldsymbol{q}$.

4 Cantilever beam Results and Discussion

The cantilever beam is fixed on the left border, and a concentrated load ($1\ KN$) is applied in the middle of the right border, as shown in Fig. 4. The dimensions for the design domain are $H = 100\ cm$ and $L = 160\ cm$, and thickness $t = 10\ mm$. It is assumed the Young's modulus $E = 100 \times 10^9\ N/m^2$ and Poisson's ratio $\upsilon = 0.3$. The structure is analyzed employing three different meshes: 32x20, 64x40 and 96x60. The parameters used in ESO

analysis is: $RR_0 = 0.1\%$, $ER = 0.1\%$ and $RC = 25\%$. The desired final volume is 45%.

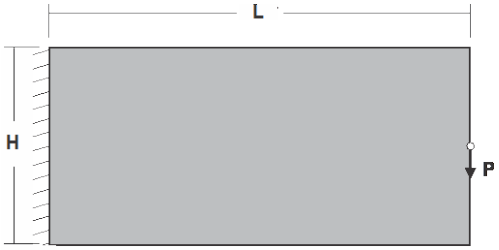

Figure 4. Cantilever beam.

Figures 5 and 6 present the results obtained in the numerical analyzes from the cantilever beam, referring to the performance parameters used, respectively, stress-based, and strain-based methods. The units of the other parameters are KN/cm² for stress, KN.cm for strain energy, and the displacements are in centimeters.
With a finer mesh, there is a reduction in the mean and standard deviation, as well as in the maximum values. A reduction in the displacement values is also noticed, where for the two cases there are similar values. The topologies present different results, indicating that for the same level of displacement stiffness, the performance parameters imply different topologies. It was verified the natural difficulty in the analyzes with the ESO to correctly define the RR0 and ER parameters that lead to an optimal structure, considering the same final volume. Hence the variation in material quantity at the end of the procedure.
Another detail refers to the checkboard pattern that is minimized when compared to the FEM, in works found in the classic ESO papers.

Meshes	Mean	S. Deviation	Maximum	Minimum	Displac.	Final Vol.	Final Topology
32x20	231.157	95.560	627.471	0.003	1.496	45.00%	
64x40	188.645	73.895	649.555	30.177	1.199	44.45%	
96x60	125.237	47.681	512.208	19.281	0.781	44.72%	

Figure 5. Optimal topologies for the cantilever beam by ESO stress-based method.

Meshes	Mean	S. Deviation	Maximum	Minimum	Displac.	Final Vol.	Final Topology
32x20	15.287	13.520	125.963	0.258	2.091	50.00%	
64x40	1.206	0.991	12.418	0.069	1.127	44.61%	
96x60	0.236	0.192	4.339	0.024	0.735	45.00%	

Figure 6. Optimal topologies for the cantilever beam by ESO strain-based method.

5 Conclusions

A new approach for Topology Optimization (TO) based on the Evolutionary Structural Optimization (ESO) via Finite-Volume Theory (FVT) is presented in this investigation. The coupling between the two techniques is possible and will serve as a basis for further studies. For example, evaluating mesh dependency, applying filtering

techniques, introducing nonlinearities, comparing results from other optimal topologies found in the literature.

Authorship statement. The authors hereby confirm that they are the sole liable persons responsible for the authorship of this work, and that all material that has been herein included as part of the present paper is either the property (and authorship) of the authors or has the permission of the owners to be included here.

References

[1] Y.M. Xie and G. P. Steven, "A Simple Evolutionary Procedure for Structural Optimization", Computers & Structures, v. 49, n. 5, pp. 885–401, 1993.
[2] L. Xia, Q. Xia, X. Huang and Y. M. Xie, "Bi-directional evolutionary structural optimization on advanced structures and materials: a comprehensive review". Archives of Computational Methods in Engineering, v. 25, n. 2, pp. 437–478, 2018.
[3] M. V. O. Araujo, E. N. Lages and M. A. Cavalcante, "Checkerboard free topology optimization for compliance minimization applying the finite-volume theory". Mechanics Research Communications, p. 103581, 2020.
[4] G. P. Steven and Y.M. Xie, "Evolutionary Topology Optimization of Continuum Structures: Methods and Applications", John Wiley & Sons, 2010.
[5] Y. Bansal, M.-J. Pindera, "Efficient reformulation of the thermoelastic higher-order theory for functionally graded materials". Journal of Thermal Stress, vol. 26, n. 11-12, pp. 1055-1092, 2003
[6] M. V. O. Araujo, E. N. Lages and M. A. A. Cavalcante. "Energy analysis of continuum elastic structures by the generalized finite-volume theory". Acta Mech 232, 4625–4643,2021.
[7] M. A. A. Cavalcante and M. J. Pindera. "Generalized finite-volume theory for elastic stress analysis in solid mechanics – part I: framework". Journal of Applied Mechanics, v. 79, n. 5, pp. 051006, 2012.
[8] M. A. A. Cavalcante and M. J. Pindera. "Generalized finite-volume theory for elastic stress analysis in solid mechanics – part II: results". Journal of Applied Mechanics, v. 79, n. 5, pp. 051007, 2012.